years) were analyzed. The inheritance pattern was considered to be autosomal dominant in 7 (18%) eyes, autosomal recessive in 9 (23%) eyes, and sporadic in 23 (59%) eyes. None of the patients was believed to have X-linked RP. The mean logMAR (logarithm of the minimum angle of resolution) best corrected visual acuity was 0.061 ± 0.069 (1.15; Snellen equivalent). The mean radius of the central visual field with the Goldmann I4e target (average value for upper, lower, nasal, and temporal directions) was 14.8° ± 12.0°.

For controls, fmERGs were recorded from 30 age-similar normal subjects (17 men, 13 women; age, 39.4 ± 16.1 years). None had known abnormalities of the visual system, and their visual acuity was 1.0 or better.

The research was conducted in accordance with the institutional guidelines of Nagoya University and conformed to the tenets of the World Medical Association's Declaration of Helsinki. Informed consent was obtained after sufficient information was provided about the examinations.

Focal Macular Electroretinograms

The stimulating and recording systems used to record the fmERGs have been described in detail.[19,20] Briefly, an infrared fundus camera equipped with a stimulus light, background illumination, and fixation target was used. The image from the camera was fed to a television monitor, and the examiner used the monitor to maintain the stimulus on the macula.

The size of the stimulus spots was selected to be 5°, 10°, and 15°, and they were centered on the fovea. The background light was delivered to the eye from the fundus camera at a visual angle of 45°. Additional background illumination outside the central 45° produced homogeneous background illumination for nearly the entire visual field. The luminances of the white stimulus light and background light were 29.46 and 2.89 cd/m^2, respectively.

A Burian-Allen bipolar contact lens electrode was used for the recordings. This lens not only allowed a very low electrical noise, but also permitted a clear view of the fundus on the monitor during the recordings.

After the patients' pupils were fully dilated with 0.5% tropicamide and 0.5% phenylephrine hydrochloride, fmERGs were elicited by 5-Hz rectangular stimuli (100-ms light on and 100-ms light off), and 512 responses were averaged by a signal processor. With this duration, the responses to the stimulus-onset was evaluated in this study, whereas the on and off responses are inseparable with the brief-flash stimuli that are widely used in the conventional full-field ERGs. A time constant of 0.03 seconds with a 100-Hz cutoff filter on the amplifier was used for recording the a- and b-waves, and a time constant of 0.003 seconds with a 300-Hz cutoff filter was used for recording the OPs.

The amplitude of the a-wave was measured from the baseline to the first negative trough, and the amplitude of the b-wave was measured from the trough of the a-wave to the positive peak of the b-wave. The amplitude of the OPs was calculated by summing the first three wavelets. The amplitudes of OPs were calculated for only the 10° and 15° stimulus spots, because the OPs elicited by the 5° spot were too small, even in normal eyes. The amplitude of the fmERG was considered to be nondetectable when it was less than the noise level (<0.4 μV).

The fmERGs elicited by this method have been shown to be generated by the cone system, and the responses elicited by spot stimuli of 5° to 15° have been shown to be local responses.[19,20]

Statistical Analyses

The significance of the differences between patients with RP and normal control subjects was analyzed using the nonparametric Mann-Whitney test. Differences in the amplitude or implicit times between 5° and 10° spots or between 10° and 15° spots were analyzed using the Wilcoxon signed rank test. Differences were considered to be significant at $P < 0.05$.

Results

Effect of Stimulus Spot Size

The fmERGs recorded from a normal subject and three representative patients with RP are shown in Figure 1. The a- and b-waves were recorded with a 0.03-second time constant (top trace) and the OPs by a 0.003-second time constant (bottom trace). Of the 39 patients with RP, only 2 had fmERG amplitudes within the normal range for all stimulus spot sizes (Fig. 1, Case 1). There were 37 patients whose fmERG amplitudes were detectable but smaller than the normal range for at least one stimulus size (Fig. 1; Case 2, Case 3).

The mean (±SD) of the amplitudes of the a-wave, b-wave, and OPs for the three stimulus spot sizes in the 39 patients with RP and 30 age-similar normal control subjects are shown in Table 1. The mean amplitudes of all ERG components were significantly smaller for all stimulus sizes in the patients with RP than in normal control subjects ($P < 0.0001$).

The amplitude of each component of the fmERGs in each patient was divided by the corresponding component of the normal control subject, and the relative data are plotted in Figure 2. We found that the degree of amplitude reduction became larger with increasing stimulus spot size for all components. The differences were statistically significant between 5° and 10° spots and between 10° and 15° spots for all components ($P < 0.05$, Fig. 2)

The mean (±SD) implicit times of all ERG components for all stimulus spots in our patients with RP and 30 age-similar normal control subjects are shown in Table 2. The data of some patients were not included in this table because it was difficult to measure their implicit time. The mean implicit times of all components in patients with RP were not significantly different from those in normal control subjects for the 5° and 10° spots, but were significantly delayed for the 15° spot except for OP3 (third positive wave of the OPs).

Waveform Changes of fmERGs in Patients with RP

We next studied the changes in the waveforms of fmERGs in our patients with RP. The amplitudes of all ERG components for the 39 patients with RP, expressed relative to the mean

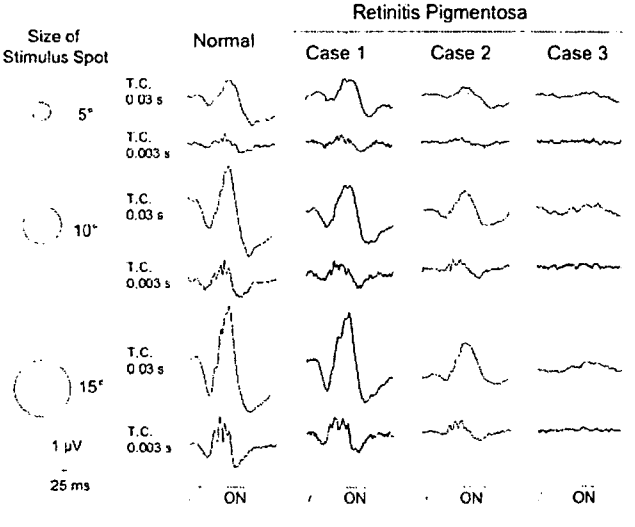

FIGURE 1. fmERGs recorded from one representative normal subject and three patients with RP. Two different time constants were used simultaneously for each recording. The a- and b-waves were recorded with a 0.03-second time constant (*top trace*) and the OPs with a 0.003-second time constant (*bottom trace*).

TABLE 1. Amplitude of Each ERG Component for Normal Control Subjects and Patients with RP

Spot Size	Waveform	Control	RP	*P*
5°	a-wave	0.59 ± 0.15	0.32 ± 0.18	<0.0001
	b-wave	1.53 ± 0.30	0.84 ± 0.38	<0.0001
10°	a-wave	1.40 ± 0.34	0.55 ± 0.28	<0.0001
	b-wave	3.52 ± 0.63	1.62 ± 0.62	<0.0001
	OPs	1.60 ± 0.43	1.08 ± 0.73	<0.0001
15°	a-wave	2.31 ± 0.56	0.83 ± 0.39	<0.0001
	b-wave	5.64 ± 0.98	2.29 ± 0.98	<0.0001
	OPs	3.17 ± 0.97	1.55 ± 1.03	<0.0001

Data are expressed as the mean ± SD. The Mann-Whitney test was used for statistical comparison.

TABLE 2. Implicit Time of Each ERG Component in Normal Control Subjects and Patients with RP

Spot Size	Waveform	Control	RP (*n*)	*P*
5°	a-wave	20.9 ± 2.6	21.6 ± 4.4 (38)	0.54
	b-wave	44.7 ± 2.9	45.2 ± 3.4 (38)	0.34
10°	a-wave	19.5 ± 1.9	21.0 ± 2.7 (39)	0.05
	b-wave	42.6 ± 3.3	44.0 ± 3.0 (39)	0.06
	OP1	24.1 ± 2.0	24.9 ± 1.9 (34)	0.09
	OP2	30.6 ± 2.1	31.6 ± 2.8 (34)	0.21
	OP3	36.8 ± 2.0	37.9 ± 3.0 (30)	0.26
15°	a-wave	19.4 ± 1.6	20.6 ± 2.7 (39)	0.02
	b-wave	40.7 ± 3.1	43.7 ± 3.0 (39)	<0.0001
	OP1	23.5 ± 1.7	24.6 ± 1.6 (36)	0.02
	OP2	30.0 ± 2.0	31.2 ± 2.3 (36)	0.04
	OP3	36.5 ± 2.2	37.2 ± 2.2 (34)	0.38

Data are expressed as the mean ± SD. The Mann-Whitney test was used for statistical comparison.

amplitudes in normal control subjects, are plotted in Figure 3. In patients with RP, the amplitudes of the OPs were better preserved than those of the b-waves for the 10° spot, and the b-waves were better preserved than the a-waves (Fig. 3A). The mean relative amplitude was 0.67 for the OPs, 0.46 for the b-wave, and 0.39 for the a-wave. The differences in the relative amplitude between these three components were statistically significant for the 10° spot ($P < 0.05$). A similar tendency was also seen for 15° spot, but the difference between the OPs and the b-wave was not significant ($P = 0.15$, Fig. 3B).

Next, we plotted the individual amplitudes of the different components of the fmERGs from the patients with RP. In Figure 4A, the amplitudes of the b-wave are plotted against the amplitudes of the a-wave elicited by the 10° spot in all 39 patients with RP and 30 normal control subjects. The shaded area shows the range of normal controls, and the dotted lines show the mean amplitudes in the normal control subjects. We found that the majority of the patients with RP (27, 69.2%) had fmERGs with amplitudes that were lower than the lowest limit of normal range for both the a- and b-waves.

The amplitudes of the OPs elicited by the 10° stimulus spot are plotted against the amplitude of the b-wave for all 39 patients with RP and 30 normal control subjects in Figure 4B. As in Figure 4A, the shaded area shows the range in the normal control subjects, and the dotted line shows the mean amplitudes in the normal control subjects.

Ten (25.6%) patients with RP had normal OP amplitudes with reduced b-wave amplitude, whereas none of the patients had normal b-wave amplitude with reduced OP amplitudes. These results combined with the data of Figure 3 indicate that the amplitudes of the OPs were better preserved than those of the b-wave for a 10° spot size in the patients with RP. We also noticed that the amplitude of OPs was larger than the upper limit of the normal range in one RP patient (Fig. 4B, arrowhead).

The fmERGs of three representative patients with RP who had a larger than normal OP/b-wave ratio are shown in Figure 5. It is clear that in these patients, the OPs were better preserved than were the a- and b-waves.

DISCUSSION

Our results showed that the degree of amplitude reduction and delay of implicit time became greater with increasing stimulus size (Tables 1, 2, Fig. 2). These results are not surprising when one considers the typical pattern of retinal dysfunction in RP. In most patients with RP, the retina is progressively impaired from the periphery to the central area. Past electrophysiological results of studies in which fERGs or mfERGs were used[5,6,10–17] are in accord with our results.

Although fERGs and mfERGs have been extensively investigated in patients with RP,[5–17] there are only a few studies in which different ERG components that originate from different retinal layers were investigated. Falsini et al.[9] analyzed the fundamental and second harmonic components of fmERGs, which are believed to originate from outer and inner retinas,

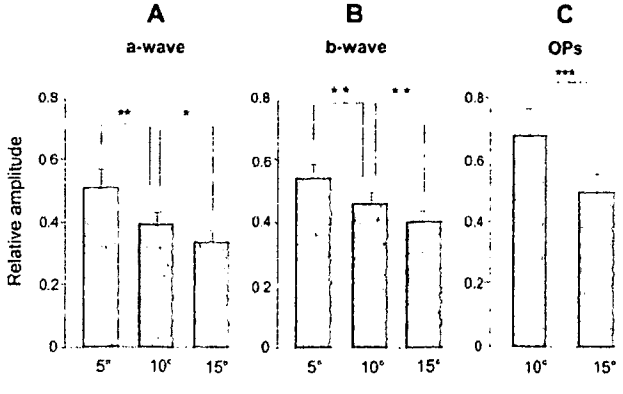

FIGURE 2. Amplitude of fmERGs in 39 patients with RP relative to the mean in normal control subjects. Comparison of the (A) a-wave and (B) b-wave amplitudes for 5°, 10°, and 15° spots. (C) Comparison of the OP amplitude for 10° and 15° spot. Bar, SEM. $^{*}P < 0.05$, $^{**}P < 0.01$, $^{***}P < 0.001$.

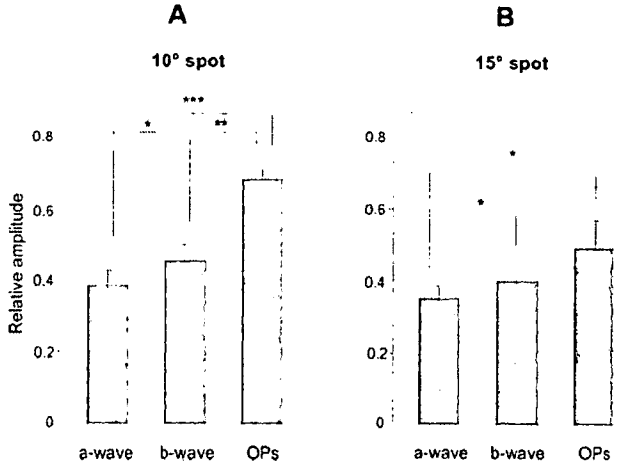

FIGURE 3. Amplitude of the fmERG in 39 patients with RP relative to the mean in normal control subjects. Comparison of the amplitude of each component for the (A) 10° and (B) 15° spot. Bar, SEM. $^{*}P < 0.05$, $^{**}P < 0.01$, $^{***}P < 0.001$.

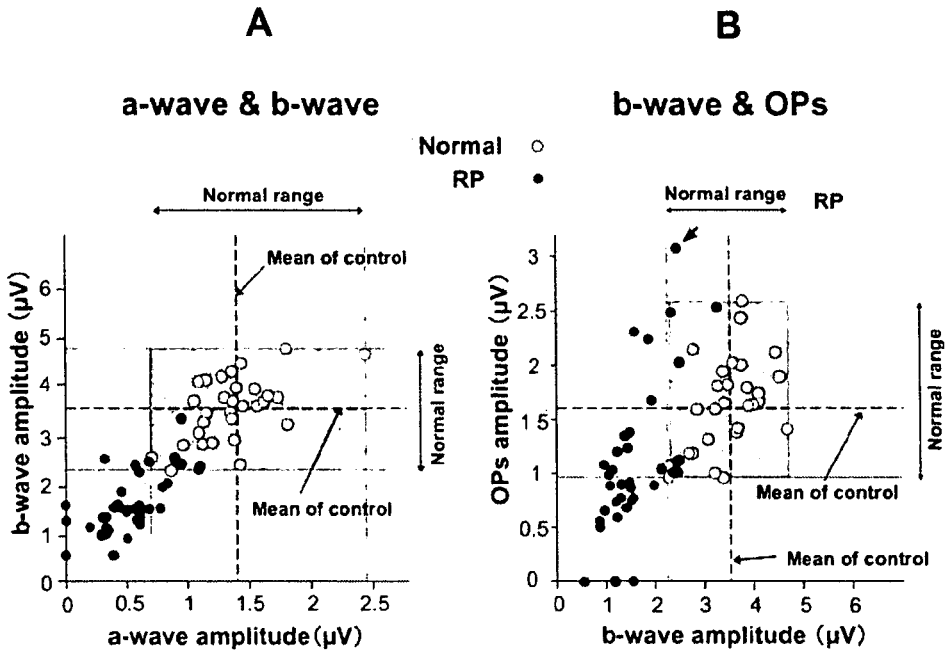

FIGURE 4. Plot of the b-wave amplitude against the amplitude of the a-wave (A), and amplitude of the OPs against the amplitude of the b-wave (B) in 30 normal subjects and 39 patients with RP. Results for the 10° stimulus spot are shown. *Shaded area*: the range of normal subjects; *dotted line*: mean of normal subjects.

respectively. They found that the ratio of the amplitudes of the fundamental component to the second harmonic component was larger in the RP group than that of normal control subjects. From these results, they concluded that not only the outer retina but also the inner retina contributed to the macular dysfunction in eyes with RP. Other ERG studies using full-field stimuli also demonstrated that neural cells postsynaptic to the photoreceptors contributed to the retinal dysfunction in eyes with RP.[21,22]

A new, interesting finding in this study was that the amplitudes of the OPs were better preserved than those of the a- and b-waves for a 10° spot in our patients with early-stage RP. The relative amplitude of the mean value in normal control subjects for the 10° spot was 0.67 for the OPs, and this value was

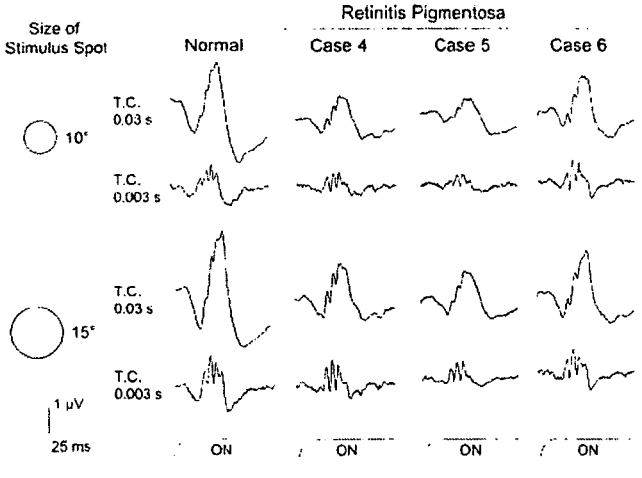

FIGURE 5. fmERGs from three patients with RP whose amplitude ratios of the OPs to the b-wave (OPs/b) are larger than the normal range for both 10° and 15° stimulus spots. Two different time constants were used simultaneously for each recording. The a- and b-waves were recorded with a 0.03-second time constant (*top*) and the OPs with a 0.003-second time constant (*bottom*). Note that the OP amplitude of Case 6 for the 10° spot is larger than the upper limit of normal control subjects (see also Fig. 4B, *arrowhead*).

significantly larger than that for the b-wave (0.46), which in turn was larger than that of the a-wave (0.39; Fig. 3A). In addition, 26% of the patients with RP had normal OP amplitudes with reduced b-wave amplitude, whereas none of the patients had normal b-wave amplitude with reduced OPs amplitudes (Fig. 4B).

Although the retinal origin of each component of fmERG has not been completely determined, one can assume their origins based on recent experiments in primates. The initial photopic a-wave is thought to originate mainly from cone photoreceptors and the cone off-bipolar cells.[23,24] The photopic b-wave is determined by the combined activities of the cone on- and off-bipolar cells.[25–27] The origins of the OPs are thought to be from feedback neural pathways in the inner part of the retina, especially around the inner plexiform layer, including the amacrine cells and partly the ganglion cells.[28–30] Recent studies[28–30] have suggested that the origins of OPs are dependent not only on individual wavelets, but also on response frequencies. Thus, our results strongly suggest that in our patients at a relatively early stage of RP, the retinal activities from the inner retinal layer (OPs) were better preserved than those from the middle and outer layers (the b- and a-waves).

The exact mechanism for the relative preservation of the macular OPs in early-stage patients with RP was not investigated in this study. We have studied the effect of stimulus intensity on the amplitude of each component of the fmERG and have found that with decreasing stimulus intensities, the a-wave, b-wave, and OPs decreased proportionally.[31] These results suggest that the waveform changes of fmERGs seen in our patients with RP cannot be explained simply by a decrease in the sensitivity to light.

The preservation of macular OPs in patients with RP is quite interesting when considering the spatial distribution of macular OPs in normal subjects. We have studied the spatial distribution of OPs in the macular area for normal subjects using an annulus (center off) stimulus to elicit fmERGs and have found that in normal subjects, the amplitude of the OPs was greater in the parafovea and perifovea. Therefore, we initially expected that the amplitudes of OPs would be more reduced

than those of the a- and b-waves for 10° and 15° spots in patients with RP, because the parafovea and perifovea was thought to be more damaged than the fovea in patients with RP. However, our results were just the opposite: The amplitudes of the OPs tended to be more preserved than those of the a- and b-waves for 10° and 15° spots in patients with RP (Fig. 3). Thus, it is interesting to consider why some patients with RP show such a selective preservation of OPs.

We have two hypotheses for the mechanism that preserves the macular OPs in patients with RP. First is the buffering effect of the large receptive fields of the OP generators, viz., the amacrine cells and ganglion cells. Histopathological studies have shown that a large percentage of the inner retinal neurons remain histologically intact even though most photoreceptors were lost in patients with RP.[32-34] Sufficient electrical activity from the inner retina may be produced by the large receptive fields, even though the electrical activities from outer and middle retinal layers are decreased as a consequence of progression of the RP. However, it is difficult to explain all the present results only by this mechanism. For example, why did one of our patients with RP (Fig. 4B, arrowhead) have supernormal OPs, despite lower borderline amplitude of the b-wave?

The second hypothesis is that the preservation of OPs in patients with RP may be due to retinal remodeling after the progressive loss of photoreceptors, to compensate for decreasing signal input to middle and inner retina. Evidence has been accumulating to support this idea in animal models of retinal degeneration.[34-40] Alman et al.[36] demonstrated that there is a compensatory synaptogenesis in reaction to partial loss of photoreceptors in rats with a rhodopsin mutation. Jones et al.[39] have shown that after loss of the outer nuclear layer, various kinds of retinal remodeling were observed not only in rodent models of photoreceptor degeneration but also in humans with RP. Our results may be a clinical demonstration that such compensatory changes can occur in some patients at the early stage of RP. However, such compensatory retinal remodeling may not occur in all patients with RP, because there was a large variation in the ratio of OPs/b-wave in our patients with RP (Fig. 4B). Such variations may be due to the different stages and severities of the disease, different genetic backgrounds, or different environmental effects.

There are some limitations to our study. First, the study was performed retrospectively, and the selection of patients was not performed randomly. Second, we did not perform molecular testing on our patients with RP and could not characterize the pattern of fmERG as a consequence of specific gene mutation. Third, we did not compare the findings of the fmERGs with detailed psychophysical results (e.g., rod and cone perimetry) or macular morphologic tests (e.g., optical coherence tomography). Further studies are needed to clarify the mechanism of the fmERGs waveform changes in patients with RP.

In conclusion, our results demonstrated that electrical activities from the inner retina are preserved better than those from middle and inner retinal layers in the central retina of patients with early-stage RP. These results can provide important information on the pathophysiology of and possible future treatment for RP.

References

1. Carr RE, Heckenlively JR. Hereditary pigmentary degenerations of the retina. In: Duane TD, Jaeger EA, eds. *Clinical Ophthalmology*. Philadelphia: JB Lippincott; 1987:1-28.
2. Heckenlively JR. RP syndromes. In: Heckenlively JR, ed. *Retinitis Pigmentosa*. Philadelphia: JB Lippincott; 1988:221-252.
3. Newsome DA. Retinitis pigmentosa, Usher's syndrome, and other pigmentary retinopathies. In: Newsome DA, ed. *Retinal Dystrophies and Degenerations*. New York: Raven Press; 1988:161-194.
4. Weleber RG, Gregory-Evance K. Retinitis pigmentosa and allied disorders. In: Hinton DR, ed. *Basic Science and Inherited Retinal Disease*. 4th ed. St. Louis: Mosby; 2006:395-498. *Retina*; vol. 1.
5. Sandberg MA, Effron MH, Berson EL. Focal cone electroretinograms in dominant retinitis pigmentosa with reduced penetrance. *Invest Ophthalmol Vis Sci*. 1978;17:1096-1101.
6. Sandberg MA, Jacobson SG, Berson EL. Foveal cone electroretinograms in retinitis pigmentosa and juvenile macular degeneration. *Am J Ophthalmol*. 1979;88:702-707.
7. Biersdorf WR. Temporal factors in the foveal ERG. *Curr Eye Res*. 1982;1:717-722.
8. Seiple W, Siegel IM, Carr RE, Mayron C. Evaluating macular function using the focal ERG. *Invest Ophthalmol Vis Sci*. 1986;27:1123-1130.
9. Falsini B, Iarossi G, Porciatti V, et al. Postreceptoral contribution to macular dysfunction in retinitis pigmentosa. *Invest Ophthalmol Vis Sci*. 1994;35:4282-4290.
10. Hood DC, Holopigian K, Greenstein V, Seiple W, Li J, Sutter EE, Carr RE. Assessment of local retinal function in patients with retinitis pigmentosa using the multi-focal ERG technique. *Vision Res*. 1998;38:163-179.
11. Chan HL, Brown B. Investigation of retinitis pigmentosa using the multifocal electroretinogram. *Ophthalmic Physiol Opt*. 1998;18:335-350.
12. Seeliger MW, Kretschmann UH, Apfelstedt-Sylla E, Zrenner E. Implicit time topography of multifocal electroretinograms. *Invest Ophthalmol Vis Sci*. 1998;39:718-723.
13. Felius J, Swanson WH. Photopic temporal processing in retinitis pigmentosa. *Invest Ophthalmol Vis Sci*. 1999;40:2932-2944.
14. Hood DC. Assessing retinal function with the multifocal technique. *Prog Retin Eye Res*. 2000;19:607-646.
15. Holopigian K, Seiple W, Greenstein VC, Hood DC, Carr RE. Local cone and rod system function in patients with retinitis pigmentosa. *Invest Ophthalmol Vis Sci*. 2001;42:779-788.
16. Vajaranant TS, Seiple W, Szlyk JP, Fishman GA. Detection using the multifocal electroretinogram of mosaic retinal dysfunction in carriers of X-linked retinitis pigmentosa. *Ophthalmology*. 2002;109:560-568.
17. Robson AG, Saihan Z, Jenkins SA, et al. Functional characterisation and serial imaging of abnormal fundus autofluorescence in patients with retinitis pigmentosa and normal visual acuity. *Br J Ophthalmol*. 2006;90:472-479.
18. Marmor MF, Holder GE, Seeliger MW, Yamamoto S. International Society for Clinical Electrophysiology of Vision. Standard for clinical electroretinography (2004 update). *Doc Ophthalmol*. 2004;108:107-114.
19. Miyake Y, Shiroyama N, Ota I, Horiguchi M. Oscillatory potentials in electroretinograms of the human macular region. *Invest Ophthalmol Vis Sci*. 1988;29:1631-1635.
20. Miyake Y. Studies of local macular ERG (in Japanese). *Acta Soc Ophthalmol Jpn*. 1988;92:1418-1449.
21. Cideciyan AV, Jacobson SG. Negative electroretinograms in retinitis pigmentosa. *Invest Ophthalmol Vis Sci*. 1993;34:3253-3263.
22. Hood DC, Birch DG. Abnormalities of the retinal cone system in retinitis pigmentosa. *Vision Res*. 1996;36:1699-1709.
23. Bush RA, Sieving PA. A proximal retinal component in the primate photopic ERG a-wave. *Invest Ophthalmol Vis Sci*. 1994;35:635-645.
24. Robson JG, Saszik SM, Ahmed J, Frishman LJ. Rod and cone contributions to the a-wave of the electroretinogram of the macaque. *J Physiol*. 2003;547:509-530.
25. Knapp AG, Schiller PH. The contribution of on-bipolar cells to the electroretinogram of rabbits and monkeys: a study using 2-amino-4-phosphonobutyrate (APB). *Vision Res*. 1984;24:1841-1846.
26. Sieving PA, Murayama K, Naarendorp F. Push-pull model of the primate photopic electroretinogram: a role for hyperpolarizing neurons in shaping the b-wave. *Vis Neurosci*. 1994;11:519-532.
27. Rangaswamy NV, Hood DC, Frishman LJ. Regional variations in local contributions to the primate photopic flash ERG: revealed

using the slow-sequence mfERG. *Invest Ophthalmol Vis Sci.* 2003; 44:3233-3247.

28. Heynen H, Wachtmeister L, van Norren D. Origin of the oscillatory potentials in the primate retina. *Vision Res.* 1985;25:1365-1373.
29. Wachtmeister L. Oscillatory potentials in the retina: what do they reveal. *Prog Retin Eye Res.* 1998;17:485-521.
30. Rangaswamy NV, Zhou W, Harwerth RS, Frishman LJ. Effect of experimental glaucoma in primates on oscillatory potentials of the slow-sequence mfERG. *Invest Ophthalmol Vis Sci.* 2006;47:753-767.
31. Shiroyama N, Miyake Y. Analysis of focal macular ERG in idiopathic central serous chorioretinopathy (in Japanese). *Nippon Ganka Gakkai Zasshi.* 1990;94:1048-1056.
32. Stone JL, Barlow WE, Humayun MS, de Juan E Jr, Milam AH. Morphometric analysis of macular photoreceptors and ganglion cells in retinas with retinitis pigmentosa. *Arch Ophthalmol.* 1992; 110:1634-1639.
33. Santos A, Humayun MS, de Juan E Jr, et al. Preservation of the inner retina in retinitis pigmentosa: a morphometric analysis. *Arch Ophthalmol.* 1997;115:511-515.
34. Milam AH, Li ZY, Fariss RN. Histopathology of the human retina in retinitis pigmentosa. *Prog Retin Eye Res.* 1998;175-205.
35. Machida S, Kondo M, Jamison JA, et al. P23H rhodopsin transgenic rat: correlation of retinal function with histopathology. *Invest Ophthalmol Vis Sci.* 2000;41:3200-3209.
36. Aleman TS, LaVail MM, Montemayor R, et al. Augmented rod bipolar cell function in partial receptor loss: an ERG study in P23H rhodopsin transgenic and aging normal rats. *Vision Res.* 2001;41: 2779-2797.
37. Banin E, Cideciyan AV, Aleman TS, et al. Retinal rod photoreceptor-specific gene mutation perturbs cone pathway development. *Neuron.* 1999;23:549-557.
38. Peng YW, Hao Y, Petters RM, Wong F. Ectopic synaptogenesis in the mammalian retina caused by rod photoreceptor-specific mutations. *Nat Neurosci.* 2000;3:1121-1127.
39. Jones BW, Watt CB, Frederick JM, et al. Retinal remodeling triggered by photoreceptor degenerations. *J Comp Neurol.* 2003;464: 1-16.
40. Marc RE, Jones BW, Watt CB, Strettoi E. Neural remodeling in retinal degeneration. *Prog Retin Eye Res.* 2003;22:607-655.

Reduction of Oscillatory Potentials and Photopic Negative Response in Patients with Autosomal Dominant Optic Atrophy with *OPA1* Mutations

Kentaro Miyata, Makoto Nakamura, Mineo Kondo, Jian Lin, Shinji Ueno, Yozo Miyake, and Hiroko Terasaki

Purpose. To study the electroretinographic (ERG) findings in patients with autosomal dominant optic atrophy (ADOA) with *OPA1* mutations.

Methods. Eight ADOA patients (age range, 24–55 years; mean, 41 years) with *OPA1* mutations were studied. In addition to routine ophthalmological tests, full-field ERGs including the rod response, mixed rod-cone response, oscillatory potentials (OPs), single-flash cone response, and photopic negative response (PhNR) were recorded and compared with those from 25 age-matched controls. The correlation between the ERG data and averaged retinal nerve fiber layer (RNFL) thickness around the optic disk measured by optical coherent tomography, mean deviation of the static perimetry (Humphrey 30-2 program), or corrected visual acuity was also examined.

Results. Amplitudes of the PhNR and OPs, both of which are believed to originate from inner retinal layers, were significantly smaller in ADOA patients than in control subjects ($P < 0.01$). Amplitudes of other ERG components were not statistically different in the two groups. OP amplitude was inversely correlated with the patient's age. The RNFL was thinner and the retinal sensitivities obtained by static perimetry were lower in ADOA patients, but these values were not correlated with the amplitude of PhNR or OPs.

Conclusions. These results suggested that there are functional impairments not only in the ganglion cell layer but also in the inner nuclear and plexiform layers, including the amacrine cells of ADOA patients with *OPA1* mutations. (*Invest Ophthalmol Vis Sci.* 2007;48:820–824) DOI:10.1167/iovs.06-0845

Autosomal dominant optic atrophy (ADOA) is the most common form of hereditary optic neuropathy. This disease is characterized by symmetrical bilateral optic atrophy associated with a decrease of visual acuity and color vision defect for blue hues.[1–6] Visual impairments usually progress slowly, and phenotypic severity varies considerably among patients even within the same family.[3–5] Histopathologic studies of donor eyes of patients with ADOA suggest that the fundamental pathologic condition is a degeneration of the retinal ganglion cells leading to optic atrophy.[7,8]

ADOA is genetically heterogeneous, and mutations of the *OPA1* gene are one of the causative genetic alterations.[9–17] The OPA1 protein is a mitochondrial dynamin-related guanosine triphosphatase (GTPase) located in the mitochondrial inner membrane space mainly anchored to the cristae of the inner membrane.[18] This protein is considered to be involved in mitochondrial fusion and in maintenance of the mitochondrial genome and network.[19–21]

It was shown that the *OPA1* gene is ubiquitously expressed in several tissues but is most abundant in the retina and brain.[10,22] Recent immunohistochemical studies in rat and mice retinas showed that the OPA1 protein was expressed predominantly in ganglion cell layer but was also expressed in the inner plexiform layer, the inner nuclear layer including the amacrine cells, and the outer plexiform layer.[20,23–25]

It is generally believed that full-field ERG findings in patients with ADOA are normal.[26,27] However, Holder et al.[28] reported that some ADOA patients had a reduction of the P50 component of the pattern ERGs thought to originate distal to the retinal ganglion cells. Because of the results of these immunohistochemical and physiological studies, we thought that a more comprehensive functional examination with the use of electroretinography should be conducted on ADOA patients with *OPA1* mutations.

We show here that the amplitudes of the photopic negative response (PhNR) and the oscillatory potential (OP), each of which is thought to originate from the inner retinal layer, were significantly reduced in the ADOA patients. Interestingly, the reduction of OPs was inversely correlated with patients' ages. These results indicated that the functions not only of the ganglion cell layer but also of the inner nuclear and inner plexiform layers are altered in the human retina with *OPA1* mutations.

Patients and Methods

Patients

Among our patients with *OPA1* gene mutations,[16] eight Japanese patients (five men and three women) from six families underwent electroretinographic examination and were recruited for this study. Detailed information on the *OPA1* gene mutations and clinical characteristics in the eight patients have been reported.[16] All the patients had typical characteristics of ADOA; one patient with an apparently atypical *OPA1* gene mutation associated with a negative ERG finding was excluded from this study.[17] The protocol of the study adhered to the tenets of the Declaration of Helsinki and was approved by the Ethics Committee of Nagoya University. Informed consent was obtained from all patients after full explanation of this study.

Clinical Examination

Ophthalmic examination included best-corrected visual acuity, slit lamp biomicroscopy, indirect ophthalmoscopy, fundus photography,

From the Department of Ophthalmology, Nagoya University Graduate School of Medicine, Nagoya, Japan.

Supported by Grants-in Aid 16591746 (MN), 16591747 (MK), and 16390497 (HT) from the Ministry of Education, Science, Sports and Culture, Japan.

Submitted for publication July 22, 2006; revised September 9, 2006; accepted November 29, 2006.

Disclosure: **K. Miyata**, None; **M. Nakamura**, None; **M. Kondo**, None; **J. Lin**, None; **S. Ueno**, None; **Y. Miyake**, None; **H. Terasaki**, None

The publication costs of this article were defrayed in part by page charge payment. This article must therefore be marked "*advertisement*" in accordance with 18 U.S.C. §1734 solely to indicate this fact.

Corresponding author: Mineo Kondo, Department of Ophthalmology, Nagoya University Graduate School of Medicine, 65 Tsuruma-cho, Showa-ku, Nagoya 466-8550, Japan; kondomi@med.nagoya-u.ac.jp.

Investigative Ophthalmology & Visual Science, February 2007, Vol. 48, No. 2

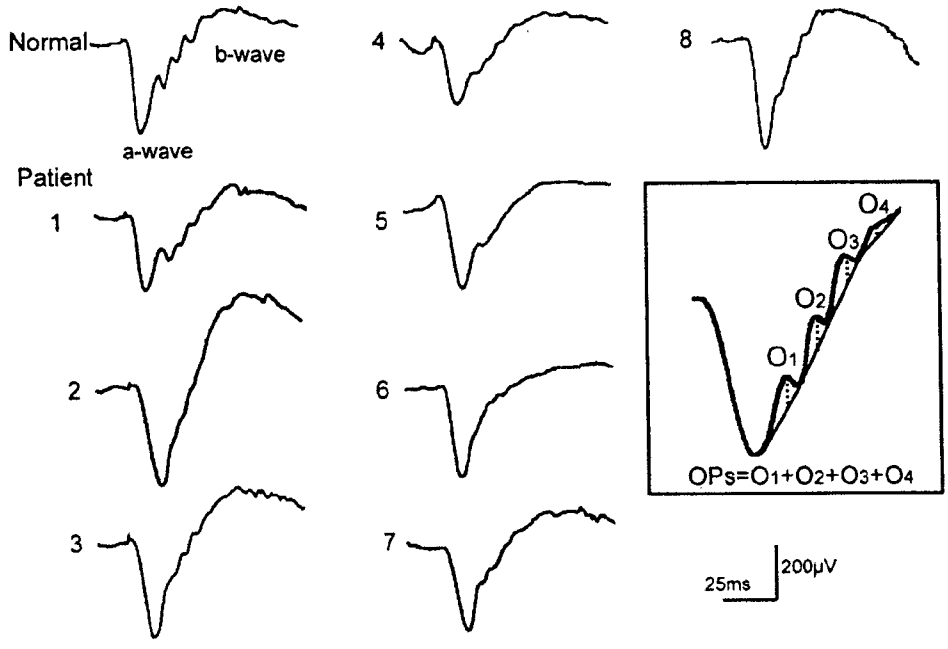

FIGURE 1. Mixed rod-cone maximal ERGs recorded from a control subject and eight ADOA patients with *OPA1* mutations. *Inset*: method used to measure OP amplitudes, expressed as the sum of the first four positive wavelets on the ascending limb of the b-wave.

visual field testing by kinetic and static perimetry, color vision testing with Farnsworth panel D-15 plates, retinal nerve fiber layer (RNFL) thickness analysis, and full-field electroretinography. Static perimetry was performed using the standard 30-2 program (size V target; Humphrey Field Analyzer; Carl Zeiss Meditec, Dublin, CA), and the mean visual field sensitivity (dB) within 30° borders of the visual field was determined. RNFL thickness was measured by optical coherence tomography (OCT-3000; Carl Zeiss Meditec) by calculating the mean RNFL thickness from 512 points around the optic disk.

Electroretinograms

Pupils were fully dilated with a combination of 0.5% tropicamide and 0.5% phenylephrine hydrochloride. Corneas were anesthetized by topical 0.4% oxybuprocaine hydrochloride before contact lens electrodes were inserted. Full-field electroretinograms (ERGs) were recorded with a Burian-Allen bipolar contact lens electrode (Hansen Ophthalmic Development Laboratories, Iowa City, IA) and Ganzfeld ERG recording system (model GS2000; LACE, Pisa, Italy). A time constant of 0.1 second and a 500-Hz high-cut filter were used.

After 30 minutes of dark adaptation, the rod response was recorded with a dim blue light at an intensity of 5.2×10^{-3} cd · s/m^2. A mixed rod-cone maximal ERG was elicited by a white flash at an intensity of 44.2 cd · s/m^2. After 10 minutes of light adaptation, a single-flash cone ERG was elicited by a white stimulus of 1.9 cd · s/m^2 on a white background of 18 cd · s/m^2.

Methods used to measure the amplitudes of the OPs and photopic negative response (PhNR) are shown in the insets of Figures 1 and 2, respectively. OP amplitudes were calculated by adding the first four positive wavelets on the ascending limb of the b-wave (Fig. 1, inset). The amplitude of the PhNR was measured from the baseline to the first negative trough after the b-wave of the single-flash cone ERG (Fig. 2, inset).

RESULTS

Clinical Findings

Clinical characteristics of the patients with *OPA1* mutations are summarized in Table 1. Visual acuities of the eight patients ranged from 0.7 to 0.01. Changes in the optic disks were symmetrical in all patients. Three patients had temporal pallor only, and in one it was subtle. The other four patients had diffuse atrophy of the optic disk. Visual field tests by Goldmann kinetic perimetry showed central scotoma in three patients (patients 1–3), concentric constriction in one patient (patient

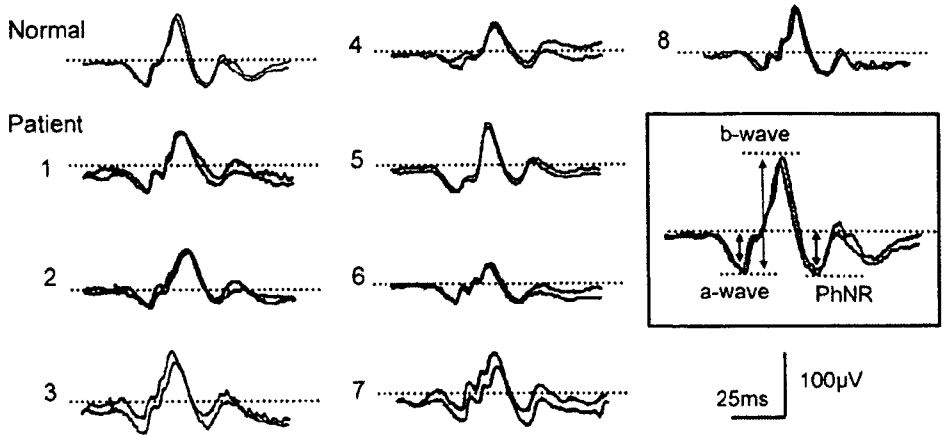

FIGURE 2. Single-flash cone ERGs recorded from a control subject and eight ADOA patients with *OPA1* mutations. *Dotted line*: baseline of the ERG response. *Inset*: method used to measure the amplitude of PhNR and the a- and b-waves.

TABLE 1. Clinical Characteristics and *OPA1* Mutations in Patients with ADOA

Patient/ Age/Sex	Family	Visual Acuity (OD/OS)	Test Eye	Disk Appearance	Humphrey Visual Field MD (dB)	RNFL Thickness (μm)	*OPA1* Mutation	PhNR (μV)	OPs (μV)
1/24/M	92	0.04/0.05	OD	DA	−20.60	29.9*	p.S545R	17.3*	144.9
2/53/F	667	0.06/0.1	OD	TP	−8.30	71.6	p.R38X	19.3*	13.8*
3/27/F	42	0.4/0/4	OD	SP	−3.15	58.7*	c.2708_2711delTTAG	20.0*	96.6
4/46/M	169	0.3/0.3	OD	DA	−5.15	64.3*	c.2538insT	20.7*	62.1*
5/50/M	169	0.3/0.3	OS	DA	−10.34	52.9*	c.2538insT	22.4	55.2*
6/51/F	247	0.01/0.01	OD	DA	Not Recorded	44.7*	p.Q61X	20.7*	41.4*
7/55/M	247	0.7/0.7	OD	TP	−2.04	66.9*	p.Q61X	25.2	62.1*
8/22/M	526	0.15/0.15	OD	TP	−3.90	68.9	c.2591insC	22.4	75.9

RNFL thickness for control subjects was 102.0 ± 16.2 μm (range, 67.8–123.0 μm). DA, diffuse atrophy; TP, temporal pallor; SP, subtle temporal pallor; MD, mean deviation.

* Lower than normal range (see also Figs. 3, 4).

6), and normal fields in four patients (patients 4, 5, 7, 8). Humphrey static perimetry showed reduced sensitivity of different degrees; mean deviation within 30° borders of the visual field ranged from -2.04 to -20.60 dB. Reliable results of static perimetry could not be obtained from one patient (patient 6) because of unstable fixation. Color vision tests using panel D-15 plates showed normal results for two patients (patients 3, 7), a minor error for one patient (patient 8), blue-yellow defects in four patients (patients 1, 2, 4, 5), and failure with no specific axis (patient 6).

The average RNFL thickness around the optic disk was 57.2 ± 16.2 μm, which was approximately 56% that of control subjects of 102.0 ± 16.2 μm (Table 1). More details about the OCT findings in ADOA patients will be presented elsewhere.

Full-Field ERGs

Rod-cone mixed maximal ERGs and single-flash cone ERGs recorded from one representative control subject and eight ADOA patients are shown in Figures 1 and 2, respectively. Mean ± SD of each ERG component for the eight ADOA patients and 25 age-matched control subjects are shown in Table 2. Differences in the amplitudes of the rod ERG b-wave, the a- and b-waves of the mixed maximal ERG, and the a- and b-wave of single-flash cone ERG were not significant in the two groups, though the average amplitudes of the a- and b-waves of the mixed maximal ERG and the a- and b-wave of single-flash cone ERG were smaller in ADOA patients than in controls.

OPs were normal in one patient (patient 1) but were clearly reduced for the other seven patients and were nearly undetectable for five patients (patients 2, 5–8; Fig. 1). The mean amplitude of OPs for ADOA patients was 69.0 ± 39.0 μV, which was approximately half that for the control subjects (155.1 ± 65.4 μV). In five of eight patients (patients 2, 4–7; Fig. 3), the amplitude of the OPs was smaller than the lower limit for control subjects.

Because the amplitudes of the a- and b-waves were slightly smaller for ADOA patients than for control subjects, we were uncertain whether the reduction in OPs resulted from an overall reduction in ERG amplitude. To examine the relationship between the OPs and the a- and b-waves, we calculated a ratio of the amplitudes of OPs to the b-wave. The mean OPs/b-wave ratio was significantly lower in ADOA patients, indicating that the reduction in the amplitude of the OPs cannot be explained by a reduction in the overall ERG ($P = 0.001$; Table 2).

The reduction in the amplitude of the OPs was also dependent on the age of the patients. The reduction in the amplitudes of the OPs as a function of age for 25 age-matched controls and eight ADOA patients are shown in Figure 3. In the control subjects, no significant correlation was observed between OP amplitude and age ($r = 0.08$; $P = 0.73$). In contrast, a significant inverse correlation was observed between OP amplitude and age ($r = -0.78$; $P = 0.02$) for the ADOA patients. It was also noted that for patients older than 40, OP amplitude was smaller than the lowest amplitude of the control subjects (Fig. 3).

The PhNR was also significantly smaller for ADOA patients (21.0 ± 2.4 μV) than for control subjects (34.3 ± 9.0 μV; $P < 0.001$; Fig. 2; Table 2). The amplitude of the PhNR in five of the eight ADOA patients was lower than the lower limit of normal in control subjects (patients 1–4, 6; Fig. 4). We also calculated the ratio of the amplitudes of PhNR to the b-wave, and this ratio was also significantly reduced for the ADOA group ($P = 0.01$; Table 2).

TABLE 2. Amplitude of Each ERG Component for Control Subjects and ADOA Patients with *OPA1* Mutations

		Mixed Rod-Cone Maximal ERG			Cone ERG		
	Rod ERG b-Wave	a-Wave	b-Wave	OP (OP/b-Wave)	a-Wave	b-Wave	PhNR (PhNR/b-Wave)
Control	132.2 ± 37.8	322.6 ± 66.4	441.0 ± 104.5	155.1 ± 65.4 (0.36 ± 0.16)	33.4 ± 8.9	94.3 ± 28.9	34.3 ± 9.0 (0.40 ± 0.18)
Patient	133.3 ± 47.4	295.0 ± 55.5	432.1 ± 88.4	69.0 ± 39.0 (0.17 ± 0.10)	28.0 ± 5.6	85.0 ± 17.1	21.0 ± 2.4 (0.26 ± 0.07)
P	0.785	0.312	0.950	0.001 (0.001)	0.074	0.400	<0.001 (0.01)

Data are expressed as mean ± SD. Mann-Whitney *U* test was used for statistical comparison. $n = 25$ control subjects; $n = 8$ patients.

No significant correlation was observed between PhNR amplitude and age for control subjects ($r = -0.32$; $P = 0.09$) and for ADOA patients ($r = -0.41$; $P = 0.32$).

Correlation between ERG Amplitudes and RNFL Thickness or Psychophysical Measurements

Mean RNFL thickness around the optic disk, visual acuity, and mean deviation of static perimetry were not significantly correlated with PhNR and OP amplitudes.

Discussion

It has generally been thought that full-field ERGs are normal in patients with ADOA[26,27] because the primary abnormality of ADOA is the degeneration of ganglion cells.[7,8] Thus, Gränse et al.[26] examined the different components of the full-field ERGs in ADOA patients with *OPA1* mutations and reported that they were within the normal range for rod and cone components. Unfortunately, they did not analyze the ERG components that originate from inner retinal layers. In 1999, Holder et al.[28] reported that the N95 component of the pattern ERG, which is thought to originate from retinal ganglion cells, was lower than the normal limit in many ADOA patients and supported the idea that the fundamental abnormality of ADOA lies in the retinal ganglion cells.

In our analysis of eight ADOA patients with *OPA1* mutations, we found that PhNR amplitudes were significantly reduced. PhNR is a negative component of the photopic ERG seen after the b-wave, and it is thought to originate mainly from the activity of ganglion cells and their axons.[29,30] PhNR amplitude is reduced after blockage of the action potentials of ganglion cells by intravitreous injection of tetrodotoxin (TTX). It is also reduced in the eyes of monkeys with experimentally induced glaucoma.[29] In clinical studies, a selective reduction of the PhNR has been reported in patients with glaucoma[30,31] and optic nerve diseases.[32] Thus, it is not surprising to find that the mean PhNR amplitude in ADOA patients was approximately two thirds that of control subjects and that the amplitudes of the PhNR in five of eight patients were lower than the lower limit of normal in control subjects. These results support the idea that PhNR can be a useful objective indicator of the function of ganglion cells and their axons.

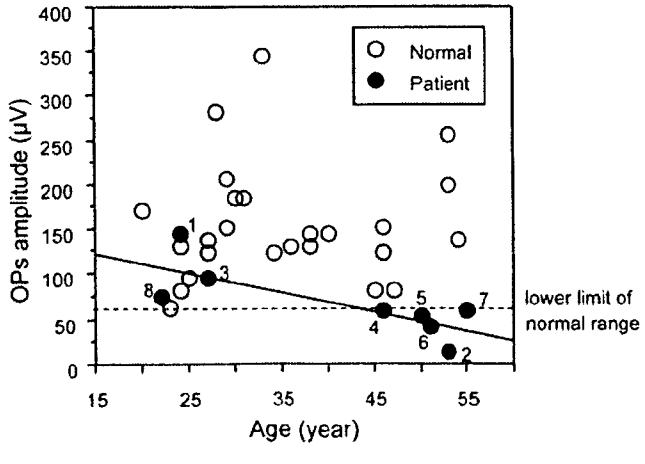

FIGURE 3. OP amplitude plotted as a function of age in 25 control subjects (○) and eight ADOA patients (●) with *OPA1* mutations. *Dotted line*: lower limit of normal range. *Solid line*: regression line between amplitude and age in the eight patients ($r = 0.78$; $P = 0.02$). The *number* shown near the ADOA patient (●) corresponds to the patient number in Table 1.

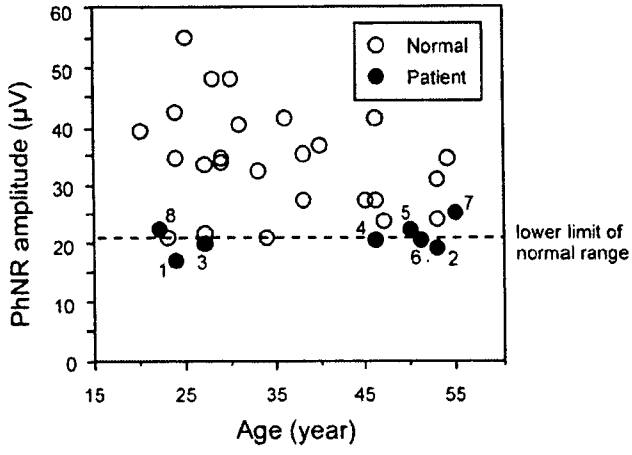

FIGURE 4. PhNR amplitude plotted as a function of age in 25 control subjects and eight ADOA patients with *OPA1* mutations. *Dotted line*: lower limit of normal range. The *number* shown near the ADOA patient (●) corresponds to the patient number in Table 1.

The most interesting finding in this study was the severe reduction in OP amplitude in ADOA patients. Thus, the mean OP amplitude in patients was less than half that in control subjects, and OP amplitude in four of eight patients was smaller than the lower limit of normal in control subjects. In addition, the strong inverse correlation between OP amplitude and age suggested progressive dysfunction of retinal neurons/circuits that gave rise to the OPs.

The origin of OPs has not been definitively determined, but OPs are generally thought to originate from feedback neural pathways in the inner retina, especially around the inner plexiform layer.[33,34] The cellular origin of OPs is thought to be mainly amacrine cells, though ganglion cells and bipolar cells may contribute to some parts of the OPs.[33-35] Our results strongly suggested that the *OPA1* gene is required not only for ganglion cell functioning but also for inner nuclear and plexiform layer—including amacrine cell—functioning. However, it is uncertain whether *OPA1* is directly related to the function of amacrine cells, where the *OPA1* gene is expressed, or whether the dysfunction of amacrine cells is secondary to ganglion cell degeneration.

Our results also indicated that the generators of the PhNR are affected severely in younger patients but that OP generators decrease slowly and progressively with age. Although the mechanism causing the gradual amplitude reduction of OPs is still undetermined, these different effects of the disease on the OPs and PhNRs may help to determine disease stage or severity.

A limitation of this study was that our patients were only relatively older patients—the youngest patient was 22—and therefore we could not analyze retinal function at earlier stages. Another limitation was that we did not record the ERGs from the same patient at different ages and thus could not state definitively the progressive nature of ADOA. Finally, our data did not differentiate whether the amplitude reduction of PhNR and OPs was specific to patients with *OPA1* mutations or more generally to optic atrophy. Further studies are needed to clarify the functional characteristics of the human retina arising from *OPA1* mutations.

References

1. Kjer P. Infantile optic atrophy with dominant mode of inheritance: a clinical and genetic study of 19 Danish families. *Acta Ophthalmol Scand.* 1959;37(suppl 54):1-146.

2. Kline LB, Glaser JS. Dominant optic atrophy: the clinical profile. *Arch Ophthalmol.* 1979;97:1680-1686.
3. Hoyt CS. Autosomal dominant optic atrophy: a spectrum of disability. *Ophthalmology.* 1980;87:245-251.
4. Votruba M, Fitzke FW, Holder GE, et al. Clinical features in affected individuals from 21 pedigrees with dominant optic atrophy. *Arch Ophthalmol.* 1998;116:351-358.
5. Johnston RL, Seller MJ, Behnam JT, et al. Dominant optic atrophy: refining the clinical diagnostic criteria in light of genetic linkage studies. *Ophthalmology.* 1999;106:123-128.
6. Miyake Y, Yagasaki K, Ichikawa H. Differential diagnosis of congenital tritanopia and dominantly inherited juvenile optic atrophy. *Arch Ophthalmol.* 1985;103:1496-1501.
7. Johnston PB, Gaster RN, Smith VC, Tripathi RC. A clinicopathologic study of autosomal dominant optic atrophy. *Am J Ophthalmol.* 1979;88:868-875.
8. Kjer P. Histopathology of eye, optic nerve and brain in a case of dominant optic atrophy. *Acta Ophthalmol.* 1982;61:300-312.
9. Delettre C, Lenaers G, Griffoin JM, et al. Nuclear gene OPA1, encoding a mitochondrial dynamin-related protein, is mutated in dominant optic atrophy. *Nat Genet.* 2000;26:207-210.
10. Alexander C, Votruba M, Pesch UE, et al. OPA1, encoding a dynamin-related GTPase, is mutated in autosomal dominant optic atrophy linked to chromosome 3q28. *Nat Genet.* 2000;26:211-215.
11. Pesch UE, Leo-Kottler B, Mayer S, et al. OPA1 mutations in patients with autosomal dominant optic atrophy and evidence for semi-dominant inheritance. *Hum Mol Genet.* 2001;10:1359-1368.
12. Toomes C, Marchbank NJ, Mackey DA, et al. Spectrum, frequency and penetrance of OPA1 mutations in dominant optic atrophy. *Hum Mol Genet.* 2001;10:1369-1378.
13. Thiselton DL, Alexander C, Morris A, et al. A frameshift mutation in exon 28 of the OPA1 gene explains the high prevalence of dominant optic atrophy in the Danish population: evidence for a founder effect. *Hum Genet.* 2001;109:498-502.
14. Delettre C, Lenaers G, Pelloquin L, et al. OPA1 (Kjer type) dominant optic atrophy: a novel mitochondrial disease. *Mol Genet Metab.* 2002;75:97-107.
15. Thiselton DL, Alexander C, Taanman JW, et al. A comprehensive survey of mutations in the *OPA1* gene in patients with autosomal dominant optic atrophy. *Invest Ophthalmol Vis Sci.* 2002;43:1715-1724.
16. Nakamura M, Lin J, Ueno S, et al. Novel mutations in *OPA1* gene and associated clinical features in Japanese patients with optic atrophy. *Ophthalmology.* 2006;113:483-488.
17. Nakamura M, Miyake Y. Optic atrophy and negative electroretinogram in a patient associated with a novel OPA1 mutation. *Graefes Arch Clin Exp Ophthalmol.* 2006;244:274-275.
18. Olichon A, Emorine LJ, Descoins E, et al. The human dynamin-related protein OPA1 is anchored to the mitochondrial inner membrane facing the inter-membrane space. *FEBS Lett.* 2002;523:171-176.
19. Olichon A, Baricault L, Gas N, et al. Loss of OPA1 perturbates the mitochondrial inner membrane structure and integrity, leading to cytochrome *c* release and apoptosis. *J Biol Chem.* 2003;278:7743-7746.
20. Kamei S, Chen-Kuo-Chang M, Cazevieille C, et al. Expression of the Opa1 mitochondrial protein in retinal ganglion cells: its downregulation causes aggregation of the mitochondrial network. *Invest Ophthalmol Vis Sci.* 2005;46:4288-4294.
21. Yoon Y, McNiven MA. Mitochondrial division: new partners in membrane pinching. *Curr Biol.* 2001;11:R67-70.
22. Misaka T, Miyashita T, Kubo Y. Primary structure of a dynamin-related mouse mitochondrial GTPase and its distribution in brain, subcellular localization, and effect on mitochondrial morphology. *J Biol Chem.* 2002;277:15834-15842.
23. Aijaz S, Erskine L, Jeffery G, et al. Developmental expression profile of the optic atrophy gene product: OPA1 is not localized exclusively in the mammalian retinal ganglion cell layer. *Invest Ophthalmol Vis Sci.* 2004;45:1667-1673.
24. Pesch UE, Fries JE, Bette S, et al. *OPA1*, the disease gene for autosomal dominant optic atrophy, is specifically expressed in ganglion cells and intrinsic neurons of the retina. *Invest Ophthalmol Vis Sci.* 2004;45:4217-4225.
25. Ju WK, Misaka T, Kushnareva Y, et al. OPA1 expression in the normal rat retina and optic nerve. *J Comp Neurol.* 2005;488:1-10.
26. Gränse L, Bergstrand I, Thiselton D, et al. Electrophysiology and ocular blood flow in a family with dominant optic nerve atrophy and a mutation in the *OPA1* gene. *Ophthalmic Genet.* 2003;24:233-245.
27. Yagasaki K, Miyake Y, Awaya S, et al. ERG (electroretinogram) in hereditary optic atrophies (in Japanese). Nippon Ganka Gakkai Zasshi 1986;90:124-130.
28. Holder GE, Votruba M, Carter AC, et al. Electrophysiological findings in dominant optic atrophy (DOA) linking to the OPA1 locus on chromosome 3q 28-qter. *Doc Ophthalmol.* 1998-99;95:217-228.
29. Viswanathan S, Frishman LJ, Robson JG, et al. The photopic negative response of the macaque electroretinogram: reduction by experimental glaucoma. *Invest Ophthalmol Vis Sci.* 1999;40:1124-1136.
30. Viswanathan S, Frishman LJ, Robson JG, Walters JW. The photopic negative response of the flash electroretinogram in primary open angle glaucoma. *Invest Ophthalmol Vis Sci.* 2001;42:514-522.
31. Colotto A, Falsini B, Salgarello T, et al. Photopic negative response of the human ERG: losses associated with glaucomatous damage. *Invest Ophthalmol Vis Sci.* 2000;41:2205-2211.
32. Gotoh Y, Machida S, Tazawa Y. Selective loss of the photopic negative response in patients with optic nerve atrophy. *Arch Ophthalmol.* 2004;122:341-346.
33. Heynen H, Wachtmeister L, van Norren D. Origin of the oscillatory potentials in the primate retina. *Vision Res.* 1985;25:1365-1373.
34. Wachtmeister L. Oscillatory potentials in the retina: what do they reveal. *Prog Retin Eye Res.* 1998;17:485-521.
35. Rangaswamy NV, Zhou W, Harwerth RS, Frishman LJ. Effect of experimental glaucoma in primates on oscillatory potentials of the slow-sequence mfERG. *Invest Ophthalmol Vis Sci.* 2006;47:753-767.

Graefe's Arch Clin Exp Ophthalmol
DOI 10.1007/s00417-006-0529-6

LETTER TO THE EDITOR

Enlargement of optic nerve resembling orbital mass in case of optic neuritis

Yumiko Ban · Hisao Ohde · Eiko Sugisaka · Kei Shinoda

Received: 19 October 2006 Revised: 9 December 2006 / Accepted: 16 December 2006

Dear Editor,

Analyses of magnetic resonance images (MRI) and cerebrospinal fluid (CSF) can provide information to make a differential diagnosis of optic neuritis from other optic nerve diseases [1, 2]. In rare cases however, those findings resemble those of optic nerve tumors [3, 4]. We present a patient with acute visual loss and an unusual swelling of the optic nerve on MRI which resembled an optic nerve tumor but was found to have optic neuritis.

A 20-year-old woman complained of a sudden decrease of vision and periorbital pain associated with ocular movements in the right eye on April 7, 2005. The visual acuity was 0.05 OD and 1.2 OS, and a right relative afferent pupillary defect was present. The anterior chamber was quiet OU. Ophthalmoscopy revealed swelling of the right optic disc, and fluorescein angiography showed hyperfluorescence of the right optic disc (Fig. 1). Goldmann perimetry showed a peripheral island in the right eye (Fig. 1).

MRI of the brain and orbits demonstrated an unusually enlarged and twisted right optic nerve (Fig. 2). The visual evoked potentials stimulating OD were abnormal. Neither neurologic evaluation nor CSF revealed any abnormalities such as myelin basic protein and oligoclonal bands.

Although an optic nerve glioma was suspected from the MRI findings, the clinical symptoms were thought to be more consistent with optic neuritis. High dose intravenous corticosteroids were given for 3 days, and the right visual acuity improved to 1.2 after 8 days. Repeat MRIs showed no abnormalities and no recurrence has been found after more than one year. Although the possibility of lymphoma or metastatic cancer could not be completely excluded, the clinical course suggested optic neuritis.

The advancements in imaging technology, e.g., fast spin-echo and the short T1 inversion recovery method in MRI, have reduced the types of diseases from which a differential diagnosis of optic neuritis must be made [2, 5]. In some cases, however, the clinical presentations are so similar to that of an optic nerve tumor that a definitive diagnosis cannot be made [2–4]. A case with classic signs of optic neuritis, but was finally diagnosed as a pilocytic astrocytoma, was reported [4].

The clinical course in our case was compatible with optic neuritis in contrast to the MR images suggesting optic nerve glioma. Although an optic nerve neoplasm may have responded to corticosteroid therapy, we believe the most probable diagnosis was optic neuritis because the patient's symptoms and signs as well as the abnormal MRI findings disappeared quickly after the treatment and no recurrence has been observed.

Differentiating optic nerve neoplasms from inflammatory changes is not necessarily easy, and metabolic, infectious, and inflammatory work-ups as well as MRI are necessary. The response to corticosteroid can help in making a definitive diagnosis, and a biopsy of the optic nerve is done only after eliminating other possibilities.

Y. Ban · H. Ohde · E. Sugisaka · K. Shinoda
Department of Ophthalmology,
Keio University School of Medicine,
35 Shinanomachi, Shinjuku-ku,
Tokyo 160-8582, Japan

H. Ohde · K. Shinoda (✉)
Laboratory of Visual Physiology, National Institute of Sensory Organs, National Hospital Organization, Tokyo Medical Center,
2-5-1 Higashigaoka, Meguro-ku,
Tokyo 152-8902, Japan
e-mail: shinodakei@kankakuki.go.jp

H. Ohde
Kamoshita Eye Clinic,
7-15-14 Roppongi, Minato-ku,
Tokyo 106-0032, Japan

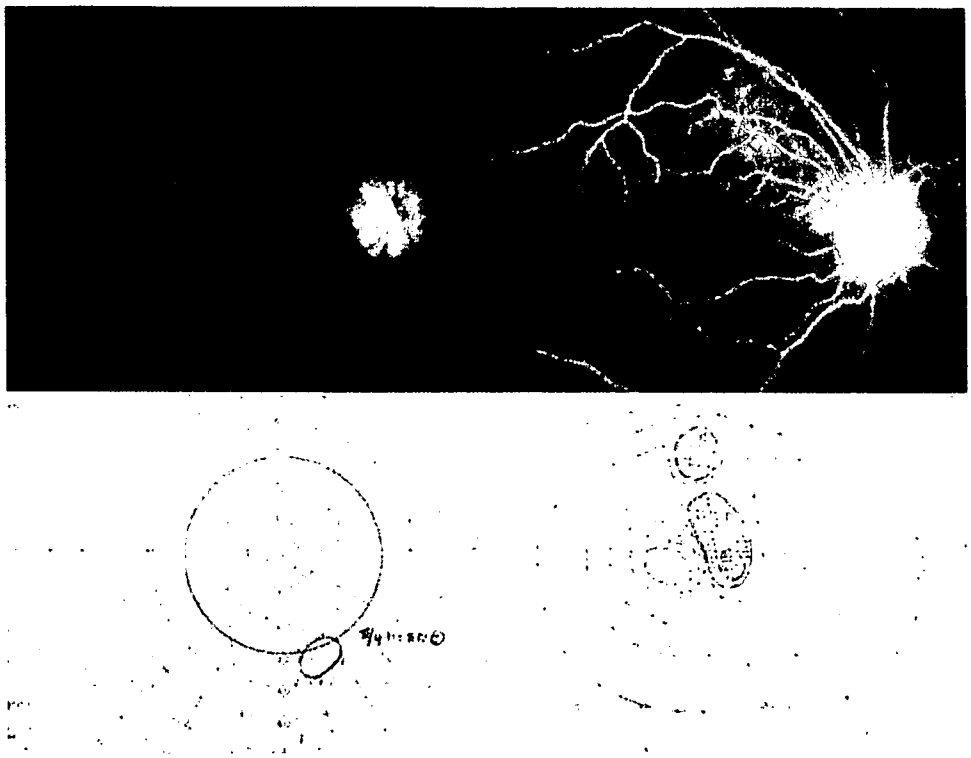

Fig. 1 Fundus photographs and visual fields of the patient's right eye. Top left. Fundus shows swelling of the right optic disc. Top right. Fluorescein fundus angiogram showing fluorescein staining of the right optic disc in the late phase. Bottom left. Goldmann visual field in the acute phase showing only a very small peripheral island in the right visual field. The corrected visual acuity was 0.01 OD. Bottom right: Goldmann visual field 19 days after high-dose intravenous corticosteroid showing a recovery in the right visual field. Visual acuity was 1.5 OD

Fig. 2 Magnetic resonance imaging (MRI) of the brain and orbits in the patient. Upper row shows MRIs in the acute phase. Upper left. T1 weighted image (T1WI) of coronal section showing a very enlarged right optic nerve. No pathological lesion was observed in other white matter or the spinal cord. Upper middle: The coronal section of MRI with the short T1 inversion recovery method showed a uniform intense gadolinium enhancement in the optic nerve that suggested that the optic nerve and not the subarachnoidal space was swollen. Upper right: T2 weighted image (T2WI) of axial section showing an unusually homogeneously enlarged and twisting right optic nerve of 7 mm diameter. The signal intensity in the right optic nerve was abnormally increased. Lower row. MRIs obtained 20 days after high-dose intravenous corticosteroid therapy. Each picture corresponds with the upper one. No abnormal findings are present in the right optic nerve compared with unaffected left optic nerve

The current findings indicate that clinicians should still consider optic neuritis in cases with MR images that suggest an optic nerve neoplasm but the symptoms are more in keeping with optic neuritis.

References

1. Beck RW, Trobe JD (1995) What we have learned from the optic neuritis treatment trial. Ophthalmology 102:1504–1508
2. Smith CH (2005) Optic neuritis. In: Miller NR, Newman NJ (eds) Walsh & Hoyt's clinical neuro-ophthalmology. vol 1, 6th edn. Williams & Wilkins, Baltimore, pp 293–348
3. Krolak-Salmon P, Androdias G, Honnorat J et al (2002) Beware of optic neuritis! Lancet Neurol 1:516–517
4. Tumialan LM, Dhall SS, Biousse V, Newman NJ (2005) Optic nerve glioma and optic neuritis mimicking one another: case report. Neurosurgery 57:E190, discussion E190
5. Gass A, Moseley IF, Barker GJ et al (1996) Lesion discrimination in optic neuritis using high-resolution fat-suppressed fast spin-echo MRI. Neuroradiology 38:317–321

Jamming of 25-gauge instruments in the cannula during vitrectomy for vitreous haemorrhage

Hajime Shinoda,[1] Takeshi Nakajima,[1] Kei Shinoda,[1,2] Kotaro Suzuki,[1] Susumu Ishida[1] and Makoto Inoue[1]

[1]Department of Ophthalmology, Keio University School of Medicine, Tokyo, Japan
[2]Laboratory of Visual Physiology, National Institute of Sensory Organs, National Organization Tokyo Medical Centre, Tokyo, Japan

ABSTRACT.

Purpose: **To report the jamming of 25-gauge instruments in the cannula during vitreous surgery for non-clearing vitreous haemorrhage.**

Methods: **Forty-five eyes underwent vitrectomy with 25-gauge instruments for non-clearing vitreous haemorrhage (VH group). The incidence of 25-gauge instruments jamming in the cannula was determined retrospectively and compared with that in 112 eyes that underwent vitrectomy for epiretinal membrane (ERM group), also using 25-gauge instruments.**

Results: **The 25-gauge vitreous cutter or light pipe became jammed in the cannula in three eyes (7%) in the VH group and the instrument locked inside the cannula had to be removed with the cannula. None of the 25-gauge instruments in the ERM group jammed ($p = 0.022$, Fisher's exact probability test). Two of three eyes developed giant retinal breaks near the sclerotomy but no retinal break related to the sclerotomy was detected in the ERM group. Examination of the cutter revealed blood trapped between the cutter and the cannula.**

Conclusions: **Twenty-five gauge instruments may become jammed in the cannula in eyes with non-clearing vitreous haemorrhage. Clinicians should be aware of this surgical complication when 25-gauge instruments are used in vitreous haemorrhage.**

Key words: 25-gauge – cannula – instrument – vitreous cutter – vitreous haemorrhage

Acta Ophthalmol. Scand.

doi: 10.1111/j.1600-0420.2007.01012.x

Introduction

The 25-gauge vitrectomy system was developed to minimize the invasiveness of vitrectomy and to permit transconjunctival sutureless vitrectomy (Fujii et al. 2002a). The initial surgical outcomes and longterm results of 25-gauge systems indicated that they were efficacious for various vitreoretinal disorders (Fujii et al. 2002b; Ibarra et al. 2005; Lakhanpal et al. 2005). However, the smaller diameter of these instruments made them more fragile, and they were more easily bent or damaged (Inoue et al. 2004). Several improvements have been made and their use has been extended to other intraocular surgical procedures (Shimada et al. 2005; Rizzo et al. 2006; Yoon et al. 2006).

The 25-gauge vitrectomy system is useful because it allows for a more tightly closed surgical field than can be achieved with the 23- or 20-gauge vitrectomy systems. This makes higher vacuum aspiration possible as a smaller amount of irrigating fluid escapes from the smaller scleral ports (Fujii et al. 2002a). To accomplish this, 25-gauge instruments are made to fit the cannula very closely, but this close fit may lead to surgical complications.

We experienced 25-gauge vitreous cutters becoming jammed in the cannula during vitreous surgery for dense vitreous haemorrhage. The incidence and possible causes of this jamming were retrospectively investigated, and the results compared with the incidence during surgery for epiretinal membrane without vitreous haemorrhage.

Materials and Methods

The 25-gauge instruments were used in 45 eyes of 39 patients who underwent vitrectomy from April 2004 to March 2006 for non-clearing, dense vitreous haemorrhages (VH group), which prevented a detailed view of the fundus by ophthalmoscopy. Informed consent was obtained from all

patients. The results from these eyes were retrospectively reviewed and compared with those from 112 eyes of 109 patients who underwent 25-gauge vitrectomy for epiretinal membrane (ERM group) during the same period. This was a consecutive series in which all surgery was performed by two of the authors (MI and HS) with similar surgical experience.

The surgeries were performed with 25-gauge vitreous cutters made by the Dutch Ophthalmic Research Center, International b. v. (DORC, International) (Zuidland, the Netherlands), Alcon Laboratories, Inc. (Fort Worth, TX, USA) and Medical Instrument Development Laboratiories (Midlabs), Inc. (San Francisco, CA, USA). The Alcon and DORC vitreous cutters are driven by Accurus (Alcon Corp.) and the Midlab cutter is driven by CV-24000 (NIDEK Corp., Nagoya, Japan). The 25-gauge cannulas were manufactured by DORC or Alcon.

The incidence of the jamming of 25-gauge instruments in the cannula was determined and possible causes investigated. Eyes that had undergone previous vitreous surgery were excluded. Statistical analysis was performed by the chi-square test, Wilcoxon's rank test and Fisher's exact probability test.

In four eyes in the VH group, the peripheral vitreous around the cannula was cut as soon as the vitreous cutter was inserted into the vitreous cavity and before the central vitreous was removed (pre-removed group). In the other 41 eyes in the VH group and all eyes in the ERM group, a routine vitrectomy procedure (i.e. removal of the central vitreous followed by removal of the peripheral vitreous) was used.

Table 1. Characteristics of the vitreous haemorrhage and epiretinal membrane groups.

	VH group	ERM group	p-value
Cases (eyes)	39 (45)	109 (112)	
Age (years)	64.8 ± 13.8	63.9 ± 12.0	0.802*
Gender (male/female)	21/18	52/57	0.577†
Cannula system (DORC/Alcon)	21/24	62/60	0.728†
Incidence of jamming (eye)	3/45	0/112	0.022†

* Wilcoxon's rank test; † Fisher's exact probability test.
VH = vitreous haemorrhage; ERM = epiretinal membrane.

Results

The mean age of the patients was 64.8 ± 13.8 years in the VH group and 63.9 ± 12.0 years in the ERM group (p = 0.802, Wilcoxon's rank test (Table 1). There were 21 men and 18 women in the VH group and 52 men and 57 women in the ERM group (p = 0.577, Fisher's exact probability test). The non-clearing vitreous haemorrhages in the VH group were caused by diabetic retinopathy in 22 eyes, branch retinal vein occlusion in 10 eyes, uveitis in four eyes, central retinal vein occlusion in three eyes, age-related macular degeneration in three eyes, rhegmatogenous retinal detachment in two eyes, and subarachnoid haemorrhage (Terson syndrome) in one eye (Table 2). Preoperative best corrected visual acuity (BCVA) in the affected eyes in the VH group was: light perception in seven eyes; hand motion in 26 eyes; counting fingers in four eyes; 0.01 in five eyes, and 0.02 in three eyes.

The cannula system manufactured by DORC International was used in 21 eyes in the VH group and 62 eyes in the ERM group; that made by Alcon was used in 24 eyes in the VH group and 60 eyes in the ERM group (p = 0.728, Fisher's exact probability test).

The 25-gauge vitreous cutter or the light pipe became jammed and/or blocked in the cannula intraoperatively in three eyes (7%) in the VH group and no eyes in the ERM group (Table 1) (p = 0.022, Fisher's exact probability test). When the instruments that jammed in the three eyes in the VH group were examined, a viscous, pigmented substance was found to be trapped in the cannula. The cutters in these cases had been made by Midlabs and Alcon (cases 29 and 30), and the light pipe by Alcon (case 33). The instruments that completely jammed in the cannula were made by Alcon (Table 2). It was impossible to either rotate or remove the cutter or the light pipe from the cannula (Fig. 1A). Thus, the jammed cannula

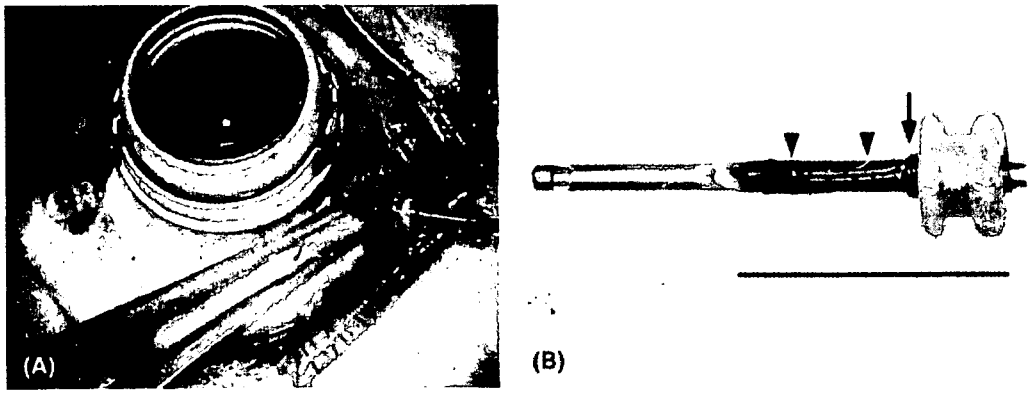

Fig. 1. (A) The 25-gauge vitreous cutter (Midlabs) jammed intraoperatively inside the cannula (Alcon) and was removed with the cannula. The inside of the cannula is black because of entrapped vitreous haemorrhage (arrow). (B) Once removed, the cutter shows haemorrhage trapped between the inner tube of the cannula and the cutter tube (arrowheads). The inner tube was folded at the plug connection (arrow) by the twisting exerted when it was removed from the cutter. (Scale bar: 5.0 mm.)

Table 2. Characteristics of cases in the vitreous haemorrhage group.

Case	Age (years)	Sex	Duration (months)	Disorder	Preop BCVA	Resistance of cannula	Cutter*	Cannula† and light pipe	Preoperative procedure‡
1	72	F	2	BRVO	0.01	–	DORC	DORC	Conv
2	49	F	6	PDR	HM	–	DORC	DORC	Conv
			2	PDR	HM	–	Alcon	Alcon	Conv
3	86	F	4	PDR	HM	–	DORC	DORC	Conv
			24	PDR	LP	–	DORC	DORC	Conv
4	51	M	1.5	PDR	HM	–	DORC	DORC	Conv
5	85	M	12	CRVO	HM	Resistant	DORC	DORC	Conv
6	60	F	1.3	Uveitis	LP	–	DORC	DORC	Conv
7	49	F	1.3	Uveitis	HM	–	DORC	DORC	Conv
			1.3	Uveitis	HM	–	DORC	DORC	Conv
8	63	M	21	PDR	LP	–	DORC	DORC	Conv
9	67	M	4.5	Terson	0.01	–	DORC	DORC	Conv
10	76	F	6	BRVO	HM	–	DORC	DORC	Conv
11	84	F	7	PDR	0.02	–	DORC	DORC	Conv
12	71	M	3	AMD	HM	–	DORC	DORC	Conv
13	74	F	1	PDR	CF	–	DORC	DORC	Conv
14	61	M	1.1	PDR	HM	–	DORC	DORC	Conv
15	74	M	3	PDR	0.01	–	DORC	DORC	Conv
			7	PDR	HM	–	Alcon	Alcon	Conv
16	84	F	2	PDR	CF	–	DORC	DORC	Conv
17	56	F	3.3	BRVO	CF	–	DORC	DORC	Conv
18	87	M	5	CRVO	LP	Resistant	DORC	DORC	Conv
19	60	F	12	PDR	HM	–	DORC	DORC	Conv
			12	PDR	0.02	–	Alcon	Alcon	Conv
20	55	F	4	PDR	0.01	–	Alcon	Alcon	Conv
21	83	M	6	BRVO	HM	–	Alcon	Alcon	Conv
22	54	F	1.8	BRVO	HM	–	Alcon	Alcon	Conv
23	74	M	2	CRVO	LP	Resistant	Alcon	Alcon	Conv
24	63	F	1	RRD	HM	–	Midlabs	Alcon	Conv
25	78	M	1.3	BRVO	0.01	–	Alcon	Alcon	Conv
26	70	M	0.9	AMD	LP	Resistant	Alcon	Alcon	Conv
27	38	F	6	PDR	HM	–	Alcon	Alcon	Pre-removed
28	68	F	12	Uveitis	HM	–	Alcon	Alcon	Conv
29	56	M	2.6	BRVO	LP	Jamming	Alcon	Alcon	Conv
30	54	M	1	BRVO	HM	Jamming	Midlabs	Alcon	Conv
31	73	M	1	AMD	HM	–	Alcon	Alcon	Pre-removed
32	61	F	1	BRVO	HM	–	Midlabs	Alcon	Pre-removed
33	64	F	6	BRVO	HM	Jamming	Midlabs	Alcon	Conv
34	68	M	0.9	RRD	HM	–	Midlabs	Alcon	Conv
35	34	M	2	PDR	HM	–	Midlabs	Alcon	Conv
36	57	M	2	PDR	HM	–	Midlabs	Alcon	Conv
			0.8	PDR	HM	–	Midlabs	Alcon	Conv
37	36	M	3	PDR	CF	–	Midlabs	Alcon	Conv
38	74	M	1	PDR	0.02	–	Midlabs	Alcon	Conv
39	62	M	2	PDR	HM	–	Midlabs	Alcon	Pre-removed

* Cutter: manufacturer of the vitreous cutter.

† Cannula: manufacturer of the cannula.

‡ Pre-removed: peripheral vitreous was removed prior to core vitrectomy; Conv: conventional vitrectomy in which peripheral vitreous was not removed prior to core vitrectomy.

M = male; F = female; BRVO = branch retinal vein occlusion; PDR = proliferative diabetic retinopathy; CRVO = central retinal vein occlusion; AMD = age-related macular degeneration; RRD = rhegmatogenous retinal detachment; BCVA = best corrected visual acuity; HM = hand motion; LP = light perception; CF = counting fingers.

had to be removed and replaced with a new cannula of the same type, and the cutter or light pipe re-inserted at the original sclerotomy site in order to continue the vitrectomy.

Retinal breaks with a localized retinal detachment were found in two of the three eyes in which instruments jammed, although none of the retinal breaks were related to the sclerotomy in the ERM group. Vitreous haemorrhage developed in these eyes as a result of branch retinal vein occlusion. These retinal breaks were located at the vitreous base where the cannula was inserted and became jammed (Fig. 2). Both eyes were treated by explanting an encircling buckle followed by gas or silicone oil tamponade.

No complications were seen in the other 42 eyes (83%) in the VH group. However, the 25-gauge vitreous cutter and light pipe were resistant to movement within the cannula in four other eyes (12%) in the VH group. In these four eyes, the surgery was successfully

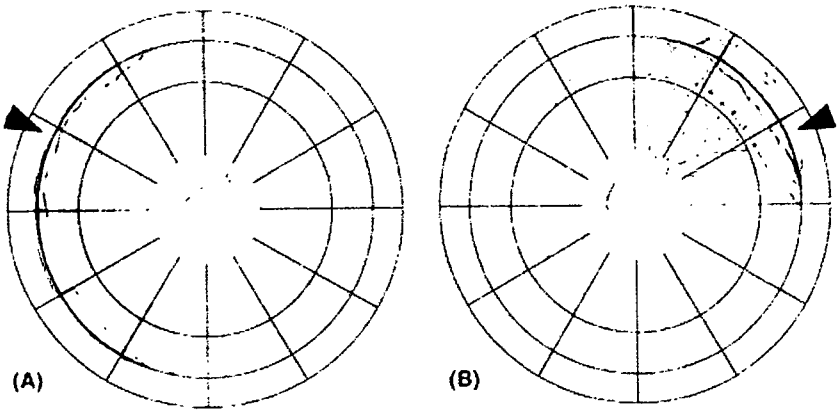

Fig. 2. Fundus charts for two patients with retinal breaks. (A) Chart for the patient in Fig. 1. The vitreous cutter was stuck inside the cannula (arrowhead) and a giant retinal break was found intraoperatively. The patient was treated with an encircling buckle and silicon oil tamponade. (B) The light pipe was stuck inside the cannula (arrowhead) and a giant retinal break was found intraoperatively. This patient was treated with encircling buckle and gas tamponade.

performed by carefully removing the peripheral vitreous around the cannula until the irrigating solution was seen to flow continuously out of the eye. The surgical instruments did not jam in the four eyes (pre-removed group) in which the peripheral vitreous around and inside the cannula had been removed before the core vitrectomy. However, because of the small number of cases in the pre-removed group, this incidence did not differ significantly from that of the conventional group ($p = 0.37$, chi-square test).

The incidence of jamming or resistance to movement in the VH group did not differ significantly between the cutters manufactured by DORC (two of 21 eyes), Alcon (three of 13 eyes) or Midlabs (two of 11 eyes) ($p = 0.41$, DORC versus Alcon; $p = 0.77$, Alcon versus Midlabs; $p = 0.48$, DORC versus Midlabs; chi-square test) or between the cannulas manufactured by DORC (two of 21 eyes) or Alcon (five of 24 eyes) ($p = 0.30$, chi-square test).

The incidence of jamming or resistance to movement did not differ significantly between the group with preoperative vision poorer than hand motion (seven of 33 eyes) and the group with VA better than finger counting (none of 12 eyes; $p = 0.08$, chi-square test). The morbidity period of visual deterioration was 6.3 ± 3.7 months in cases in which the instruments jammed or were resistant and 4.5 ± 3.6 months in cases in which the instruments did not jam or become resistant ($p = 0.86$, unpaired *t*-test).

Discussion

The 25-gauge vitrectomy system was initially designed to decrease the surgical invasiveness of peripheral vitrectomy. However, refinements in the instruments and techniques have expanded their surgical use (Shimada et al. 2005). To increase the efficiency of smaller diameter instruments, the cannula was made to fit the diameter of the instruments more closely (Fujii et al. 2002a). The inner diameter of the DORC cannula is 0.53 mm and that of the Alcon 0.54 mm. However, in outer diameter, the DORC vitreous cutter measures 0.51 mm and the Alcon and Midlabs cutters measure 0.52 mm, according to the specifications given in their respective catalogues. This tight fit results in a decrease in the leakage of intraocular irrigating fluid, which should stabilize intraocular pressure during vitrectomy with high-vacuum aspiration (Fujii et al. 2002a).

However, when dense vitreous haemorrhage is removed during vitrectomy, the thick haemorrhage and condensed peripheral vitreous around the cannula may become trapped in the inner tube of the cannula by repeated movements of the vitreous cutter or light pipe through the cannula. This phenomenon was not specific to the cannula system of a particular manufacturer, as we had similar experiences with both the Alcon and DORC cutters. However, a higher incidence was found in eyes with poorer preoperative vision or with a longer postoperative morbidity period of visual deterioration. One of the reasons for this may be that preoperative vision may be correlated with the degree of condensed vitreous or blood clots. However, we were unable to determine the significance of this hypothesis because of the small number of eyes.

Once the vitreous cutter is jammed in the cannula, the cannula may damage the sclerotomy site, resulting in possible peripheral retinal breaks or oral dialysis. Electromicroscopic examinations have revealed the entrapment of vitreous at the sclerotomy site after conventional vitrectomy (Koch et al. 1995). However, biomicroscopic analyses revealed no significant difference between conventional vitrectomy and sutureless 25-gauge vitrectomy (Kwok et al. 2001). The trapped vitreous with haemorrhage at the cannula may cause peripheral retinal breaks as well as the entrapment of vitreous at the sclerotomies (Liu et al. 2004; Wimpissinger & Binder 2007).

Conclusions

Clinicians should be aware that 25-gauge instruments may become jammed in the cannula when surgerys is performed in eyes with non-clearing vitreous haemorrhage or thickened vitreous. To avoid this, we recommend the removal of vitreous around the cannula prior to central vitrectomy, especially in eyes with massive vitreous haemorrhage with poorer preoperative vision and a longer morbidity period of visual deterioration. Because of the small number of eyes included in this study, further prospective randomized studies to evaluate the efficacy of these surgical instruments are needed.

References

Fujii GY, De Juan E Jr, Humayun MS, Chang TS, Pieramici DJ, Barnes A & Kent D (2002b): Initial experience using the

transconjunctival sutureless vitrectomy system for vitreoretinal surgery. Ophthalmology **109**: 1814–1820.

Fujii GY, De Juan E Jr, Humayun MS et al. (2002a): A new 25-gauge instrument system for transconjunctival sutureless vitrectomy surgery. Ophthalmology **109**: 1807–1812.

Ibarra MS, Hermel M, Prenner JL & Hassan TS (2005): Longer-term outcomes of transconjunctival sutureless 25-gauge vitrectomy. Am J Ophthalmol **139**: 831–836.

Inoue M, Noda K, Ishida S, Nagai N, Imamura Y & Oguchi Y (2004): Intraoperative breakage of a 25-gauge vitreous cutter. Am J Ophthalmol **138**: 867–869.

Koch FH, Kreiger AE, Spitznas M, Glasgow B, Foos RY & Yoshizumi MO (1995): Pars plana incisions of four patients: histopathology and electron microscopy. Br J Ophthalmol **79**: 486–493.

Kwok AK, Tham CC, Loo AV, Fan DS & Lam DS (2001): Ultrasound biomicroscopy of conventional and sutureless pars plana sclerotomies: a comparative and longitudinal study. Am J Ophthalmol **132**: 172–177.

Lakhanpal RR, Humayun MS, de Juan E Jr et al. (2005): Outcomes of 140 consecutive cases of 25-gauge transconjunctival surgery for posterior segment disease. Ophthalmology **112**: 817–824.

Liu W, Huang SY, Zhang P, Tang SB, Li JQ & Zheng HL (2004): Bioptic significance of incarcerated contents at sclerotomy sites during vitrectomy. Retina **24**: 407–411.

Rizzo S, Genovesi-Ebert F, Murri S, Belting C, Vento A, Cresti F & Manca ML (2006): 25-gauge, sutureless vitrectomy and standard 20-gauge pars plana vitrectomy in idiopathic epiretinal membrane surgery: a comparative pilot study. Graefes Arch Clin Exp Ophthalmol **244**: 472–479.

Shimada H, Nakashizuka H, Mori R & Mizutani Y (2005): Expanded indications for 25-gauge transconjunctival vitrectomy. Jpn J Ophthalmol **49**: 397–401.

Wimpissinger B & Binder S (2007): Entry-site-related retinal detachment after pars plana vitrectomy. Acta Ophthalmol Scand (in press).

Yoon YH, Kim DS, Kim JG & Hwang JU (2006): Sutureless vitreoretinal surgery using a new 25-gauge transconjunctival system. Ophthalmic Surg Lasers Imaging **37**: 12–19.

Received on May 4th, 2007.
Accepted on June 19th, 2007.

Correspondence:
Makoto Inoue MD
Department of Ophthalmology
Keio University School of Medicine
35 Shinanomachi, Shinjuku
Tokyo 160-582
Japan
Tel: + 81 3 3353 1211 ext. 62402
Fax: + 81 3 3359 8302
Email: inoshin@sc.itc.keio.ac.jp

Visual recovery after vitrectomy for macular hole using 25-gauge instruments

Hajime Shinoda,[1] Kei Shinoda,[1,2] Shingo Satofuka,[1] Yutaka Imamura,[1] Yoko Ozawa,[1] Susumu Ishida[1] and Makoto Inoue[1]

[1]Department of Ophthalmology, Keio University School of Medicine, Tokyo, Japan
[2]Laboratory of Visual Physiology, National Institute of Sensory Organs, National Organization Tokyo Medical Centre, Tokyo, Japan

ABSTRACT.

Purpose: **To determine whether vitrectomy with 25-gauge instruments contributes to better postoperative visual recovery after macular hole (MH) surgery.**

Methods: **The medical records for 46 consecutive eyes operated for MH by a single surgeon were retrospectively examined. Vitrectomy had been performed with a 25-gauge instrument in 23 eyes (25-G group) and with a 20-gauge instrument in 23 eyes (20-G group). Postoperative visual acuity (VA) in logMAR (logarithm of the minimum angle of resolution) units after 1 week and 1, 3, 6, 9 and 12 months, operating time, and volume of intraocular irrigating fluid were compared between the two groups.**

Results: **Mean preoperative logMAR VA was 0.72 in the 25-G group and 0.68 in the 20-G group ($p = 0.282$, unpaired *t*-test). One week after surgery, VA was significantly better in the 25-G group (0.40 ± 0.34) than in the 20-G group (0.58 ± 0.30) ($p = 0.020$). This significant difference was maintained until 9 months after surgery, but was no longer evident at 12 months ($p = 0.182$). Operating time was significantly shorter in the 25-G group (56 ± 16 mins) than in the 20-G group (85 ± 28 mins) ($p = 0.003$, unpaired *t*-test). The volume of intraocular irrigating fluid was significantly less in the 25-G group (244 ± 72 ml) than in the 20-G group (416 ± 113 ml) ($p < 0.0001$).**

Conclusions: **The use of 25-gauge vitrectomy instruments leads to better postoperative visual recovery following surgery for MH during the first 9 months, probably as a result of shorter surgical time and a lower volume of intraocular irrigating fluid.**

Key words: 25-gauge vitrectomy – macular hole – postoperative recovery – postoperative complications

Acta Ophthalmol. Scand.

doi: 10.1111/j.1600-0420.2007.01000.x

Introduction

Twenty-five gauge surgical instruments were introduced for vitreal surgery in 1990 to facilitate delicate vitreoretinal dissections, particularly at the vitreous base and when fibrovascular tissues were closely adherent to the retina (De Juan & Hickingbotham 1990). Because of their smaller size, these instruments were more precise in their cutting capabilities than other instruments (De Juan & Hickingbotham 1990). Further improvements were made in the instruments, with the development of a 25-gauge transconjunctival sutureless vitrectomy system (Millennium TSV25™; Baush & Lomb, NY, USA) to replace 20-gauge instruments in selected cases because they were considered less invasive (Fujii et al. 2002a, 2002b). Recent analyses have shown the longterm results after 25-gauge vitrectomy to be effective and safe (Ibarra et al. 2005; Lakhanpal et al. 2005). The recent improvements in 25-gauge vitreous instruments have expanded the indications for 25-gauge vitreous surgeries (Shimada et al. 2005).

The 25-gauge vitreous system uses smaller incisions that allow transconjunctival sutureless sclerotomies, which has led to a reduction in postoperative corneal astigmatism. In addition, the volume of intraocular irrigating fluid used during 25-gauge vitrectomy is believed to be less than that required with the 20-gauge system. These differences between the 25- and 20-gauge instruments should make visual recovery better with the 25-gauge system, but this has not been quantified for macular hole (MH) surgery. Thus, the purpose of this study was to compare postoperative visual events after MH surgery with 25- and 20-gauge instruments.

Materials and Methods

The medical records of 46 consecutive eyes which had undergone vitrectomy with 25- or 20-gauge vitrectomy instruments for an MH, carried out by a single surgeon (MI), and which had been followed for at least 1 year were examined. All patients were fully informed about the treatment protocol and gave signed informed consent. The patients were not randomly divided into the two treatment groups. We used 20-gauge vitrectomy in the early period and then changed to 25-gauge vitrectomy for macular hole surgery. Thus, these two groups were divided by the earlier and later periods. The procedures used conformed to the tenets of the Declaration of Helsinki.

The 25-gauge vitrectomy system (DORC International, Zuidland, the Netherlands) was used in 23 eyes (25-G group) and the 20-gauge vitrectomy system (1500 cutter; Alcon Corp., Fort Worth, TX, USA) was used in 23 eyes (20-G group). Simultaneous cataract surgery was performed if the lens was even mildly cataractous to avoid postoperative progression of a nuclear cataract. Patients with more than moderate cataract (> 3 Emery grade) were excluded.

The surgical procedures were similar for both systems. The inner limiting membrane (ILM) was removed without indocyanine green or triamcinolone acetonide staining in all cases. A triangular flap was created by gasping the ILM with an end-gripping forceps (20-G or 25-G; DORC International) and peeling it off circumferentially for approximate 2 disc diameters (DD) around the macular hole. The peeling was performed in a manner similar to that used in the continuous curvilinear capsulorhexis of the anterior lens capsule process during cataract surgery. The border between the peeled and unpeeled areas was identified by a wrinkled reflex on the retinal nerve fibre layer.

Peripheral vitreous was removed through the ora serrata in each group with scleral indentation and endophotocoagulation was applied if peripheral retinal breaks were present. The surgery was completed with an exchange of air for vitreous fluid. In the eyes with peripheral retinal breaks, 10% SF6 gas was injected for tamponade. The patients were instructed to maintain a facedown position for 3 days. In two eyes with peripheral retinal breaks, the 25-G sclerotomy was enlarged to 20-G in order to insert a 20-G endolaser probe with endoillumination. These sclerotomies were sutured in the usual manner. Sutures were not used in any other eyes in the 25-G group, including those eyes with retinal breaks treated with a 25-G endolaser probe.

The two groups were compared for patient age, morbidity period, stage of macular hole and observation period. The stage and closure of the macular hole was confirmed by ophthalmoscopy and optical coherence tomography (OCT). Preoperative best corrected visual acuity (BCVA) in logMAR units (logarithm of the minimum angle of resolution) was compared with postoperative BCVA after 1 week and 1, 3, 6, 9 and 12 months. In addition, operating time, volume of intraocular irrigating balanced salt solution (BSS) plus surgery-induced astigmatism (i.e. postoperative astigmatism subtracted from preoperative astigmatism, obtained at the same axis using an autorefractometer [ARK-700 A; Nidek Co., Ltd, Aichi, Japan]) were compared. The incidence of peripheral retinal breaks including sclerotomy-related retinal breaks was evaluated. Sclerotomy-related retinal breaks were defined as oral dialysis or peripheral retinal breaks located at the vitreous base close to the sclerotomy.

Statistical analyses

Unpaired *t*-test or chi-square test was used for statistical analysis. A p-value < 0.05 was defined as statistically significant.

Results

Preoperative values

The demographics of patients in the two groups are presented in Table 1. Their mean age was 64.7 ± 6.4 years in the 25-G group and 67.5 ± 7.1 years in the 20-G group ($p = 0.200$) (Table 1). The preoperative stage of macular hole did not differ significantly between the two groups ($p = 0.809$). Simultaneous cataract surgery was performed in 20 eyes in the 25-G group and 18 eyes in the 20-G group ($p = 0.437$). The morbidity period was 2.6 months in the 25-G group and 3.2 months in the 20-G group ($p = 0.504$).

Macular hole closure

The macular hole was closed after the first surgery in 22 of 23 eyes in the 25-G group (96%) and 22 of 23 eyes in the 20-G group (96%). This difference was not significant ($p > 0.999$, chi-square test). In the two eyes in which the macular hole was not closed, the hole was successfully closed by a second surgery. The additional surgery was performed with the 25-gauge vitrectomy system in the 25-G group and with the 20-gauge vitrectomy system in the 20-G group.

Visual acuity

The mean preoperative logMAR vision was 0.72 in the 25-G group and 0.68 in the 20-G group ($p = 0.282$) (Table 1). At 1 week, postoperative vision could be measured through a residual gas bubble in all eyes, and the mean postoperative logMAR VA improved to 0.40 ± 0.34 in the 25-G group and 0.58 ± 0.30 in the 20-G group (Fig. 1, Table 2). At 1 month, mean

Table 1. Preoperative values in both groups.

		25-G group	20-G group	p-value
Age (years)		64.7 ± 6.4	67.5 ± 7.1	0.200*
Morbidity period (months)		2.6 ± 7.8	3.2 ± 4.2	0.504*
Stage of macular hole	I	0	0	0.809†
	II	6	5	
	III	16	16	
	IV	1	2	
Preoperative VA (logMAR)		0.72 ± 0.36	0.68 ± 0.27	0.282*
Simultaneous cataract surgery		20 (87%)	18 (78%)	0.437†
Observation period (months)		17.3 ± 2.7	19.8 ± 6.8	0.096*

* p-value according to unpaired *t*-test.
† p-value according to chi-square test.
VA = visual acuity.